Journal of Inorganic and General Chemistry
ZAAC
Zeitschrift für anorganische und allgemeine Chemie
DOI: 10.1002/zaac.202100066
ARTICLE

An Iron-Hydrogen Bond Resistant to Protonation and Oxidation

Joel D. Collett,[a] Rebecca W. Ransohoff,[a] Jeanette A. Krause,[a] and Hairong Guan*[a]

A new synthetic route to *cis*-(^{Cy}PNP)Fe(CO)$_2$H (^{Cy}PNP = 2,5-bis(dicyclohexylphosphinomethyl)pyrrolyl) has been developed, involving the reaction of (^{Cy}PNP)Fe(CO)$_2$Br with $NaBH_4$. The Fe–H bond of this iron hydride is remarkably stable to acids (e.g., $HBF_4 \cdot Et_2O$, HCl, and CH_3CO_2H) and oxidants (e.g., 1,4-benzoquinone and galvinoxyl), only leading to the protonation of the β-pyrrolic carbon and the oxidation of the ligand backbone, respectively. Under 369 nm UV irradiation, *cis*-(^{Cy}PNP)Fe(CO)$_2$H has been shown to react with ethylene to yield *cis*-(^{Cy}PNP)Fe(CO)$_2$Et and undergo H/D exchange with C_6D_6 to form *cis*-(^{Cy}PNP)Fe(CO)$_2$D and C_6D_5H. Both processes likely proceed via an initial CO dissociation step to yield (^{Cy}PNP)Fe(CO)H as a reactive intermediate.

Introduction

The first iron hydride complex, $H_2Fe(CO)_4$, was reported by Hieber and Leutert in 1931,[1] and since then many other iron hydrides have been synthesized for a wide variety of applications. In particular, iron hydrides can serve as catalysts or catalytic intermediates in hydrogenation, hydrosilylation, hydroboration, and C–C bond forming reactions as well as electrochemical or photochemical reduction of H^+ to H_2.[2] Given that iron is an inexpensive, earth-abundant, and environmentally benign metal, it is not surprising to see iron-based catalysts being developed in both academic and industrial labs. This would require in-depth reactivity studies of well-defined iron hydrides.

Of the ligands used to stabilize iron hydride species, pincer ligands (or tridentate, meridionally coordinating ligands) have proved to be very successful, in part due to their strong chelation to iron.[3] The high tunability of the pincer scaffold also provides ample opportunities to modulate the reactivity of the Fe–H bond. One specific type of pincer ligand that stands out in iron catalysis involves a central nitrogen donor flanked by two phosphine-based pincer arms, which is often described as a PNP-pincer ligand. The nitrogen donor can be part of an aromatic ring (e.g., pyridine)[4] or an aliphatic chain with $HN(CH_2CH_2PR_2)_2$ being studied the most.[5]

This work focuses on a PNP-pincer ligand bearing a deprotonated pyrrole ring as illustrated in Figure 1 (abbreviated here as ^{Cy}PNP). Its phenyl derivative, ^{Ph}PNP, was reported first in 2012 by Gade,[6] Mani,[7] and Tonzetich,[8] independently, in their studies of nickel pincer complexes. As far as iron hydrides are concerned, "(^{Cy}PNP)FeH" has been shown to adopt a dimeric structure with the ^{Cy}PNP ligand (μ-κ^2-P,N:κ^1-P) and the hydride bridging two iron centers.[9] The dimerization can be suppressed in the presence of another coordinating ligand such as CO,[9a] 2,2′-bipyridine,[10] or $PhPMe_2$,[11] or using a sterically more hindered PNP-pincer ligand like ^{tBu}PNP.[12] We have been particularly interested in *cis*-(^{Cy}PNP)Fe(CO)$_2$H (**1**) reported by Tonzetich and co-workers.[9a] This specific iron hydride closely resembles our previously studied *cis*-(^{iPr}POCOP)Fe(CO)$_2$H (^{iPr}POCOP = 2,6-bis(diisopropylphosphinito)phenyl) for catalytic hydrosilylation reactions.[13] While **1** was pronounced "too cold" due to its lack of reactivity towards alkenes and CO_2,[9a,10] we discovered some intriguing reaction patterns with this compound that are not typical of an iron hydride. These results are described in detail here.

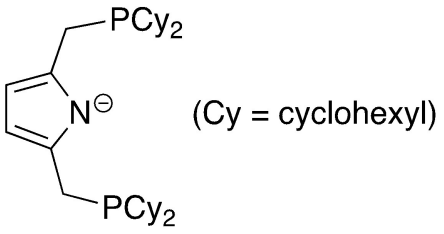

Figure 1. The PNP-pincer ligand used in this study.

Results and Discussion

The iron hydride **1** was previously prepared according to the following procedure: treatment of Na(^{Cy}PNP) with $FeCl_2(THF)_{1.5}$ in the presence of pyridine (pyr) afforded (^{Cy}PNP)Fe(pyr)Cl, which was then allowed to react with $NaBEt_3H$ under a CO atmosphere.[9a] We developed a more convenient and higher-yielding route that involved the reaction of Li(^{Cy}PNP)[14] with

[a] J. D. Collett, R. W. Ransohoff, J. A. Krause, Prof. H. Guan
Department of Chemistry
University of Cincinnati
P.O. Box 210172
Cincinnati, Ohio 45221-0172
United States
Fax: +1-513-556-9239
E-mail: hairong.guan@uc.edu

Supporting information for this article is available on the WWW under https://doi.org/10.1002/zaac.202100066

$FeBr_2$ under CO followed by the addition of $NaBH_4$ (Scheme 1). To minimize the reduction of the metal center, it is important to add $NaBH_4$, in two portions, to a chilled reaction mixture. The isolated product spectroscopically matches the one reported in the literature,[9a] although the color is significantly lighter (pale green vs. blue).[15] The structure was further confirmed by X-ray crystallography (see Supporting Information).

Efforts were made to isolate the complex from the first step of the synthesis outlined in Scheme 1. Interestingly, a short reaction time (5–15 min) always led to the isolation of (^{Cy}PNP)$Fe(CO)_2Br$ as a mixture of *cis* and *trans* isomers. Extending the reaction time to >1 h gave rise to *cis*-(^{Cy}PNP)$Fe(CO)_2Br$ (**2**) only, suggesting that the *trans* isomer is a kinetic product. Presumably, the *trans*-to-*cis* isomerization is driven by the avoidance of having the strongly *trans*-influencing CO ligand *trans* to another CO ligand. The presence of two inequivalent CO ligands in **2** was established by X-ray crystallography (see Supporting Information) and $^{13}C\{^1H\}$ NMR spectroscopy which, in C_6D_6, showed two triplets at 216.1 ppm ($J_{C\text{-}P}=23.9$ Hz) and 215.0 ppm ($J_{C\text{-}P}=15.6$ Hz). Irradiation of **2** with 369 nm UV light generated *trans*-(^{Cy}PNP)$Fe(CO)_2Br$ (**3**), but under thermal conditions **3** was reverted back to **2** (Scheme 2). Repeating this experiment under ^{13}CO (1 bar) produced a mixture of **3**, **3-^{13}CO**, and **3-(^{13}CO)$_2$**, as judged by the appearance of a new singlet, doublet, and triplet (overlapped) in the $^{31}P\{^1H\}$ NMR spectrum. The photogenerated **3-^{13}CO** and **3-(^{13}CO)$_2$** (in C_6D_6) displayed only one triplet at 218.2 ppm ($J_{C\text{-}P}=23.2$ Hz) for the ^{13}CO resonance,[16] consistent with the C_{2v} symmetry for the *trans* isomer. This ^{13}C-enriched mixture eventually isomerized to **2**, **2-^{13}CO**, and **2-(^{13}CO)$_2$** after the UV light source was removed.

As expected, the reaction of the isolated bromide complex (pure **2** or a mixture of **2** and **3**) with $NaBH_4$ also yielded the iron hydride **1**. This result stands in contrast to the reported reaction of *cis*-(^{Cy}PNP)$Fe(CO)_2Cl$ with $NaBEt_3H$, which formed an Fe(I) species (^{Cy}PNP)$Fe(CO)_2$.[9a] Reduction of Fe(II) by the borohydride must occur when the halide remains bound to iron. A homolytic cleavage of the Fe–H bond leading to the decomposition of **1** to (^{Cy}PNP)$Fe(CO)_2$ and H_2 is unlikely, as the iron hydride (under argon) is stable at ambient temperature for an extended period of time.

The iron hydride **1** lacks the reactivity typically anticipated for a transition metal hydride. At room temperature, aldehydes, ketones, esters, CO_2 (1 bar), and alkenes were shown to be unreactive towards **1**, an observation that was also made by Tonzetich and co-workers.[9a,10] In case this is due to a thermodynamic phenomenon, a solution of **1** in C_6D_6 was treated with deuterium-labelled benzaldehyde (PhCDO). No H/D exchange was observed in 24 h, confirming that the insertion process is kinetically unfavorable. Additionally, **1** proved to be stable to water and did not produce H_2 when mixed with acids.

Under more forcing conditions (100 °C, in toluene, $p_{H2}=$ 40 bar, 24 h), **1** (3 mol% catalyst loading) remained inactive for catalytic hydrogenation of PhCHO, $PhCOCH_3$, and $PhCO_2Me$. However, in the presence of $HBF_4\cdot Et_2O$ (3 mol%) as an additive, ~5 mol% of PhCHO was hydrogenated to $PhCH_2OH$. This prompted us to further examine the stability of **1** towards acids.

A stoichiometric reaction between **1** and $HBF_4\cdot Et_2O$ was thus carried out in C_6D_6, resulting in an immediate color change from pale green to yellow. The $^{31}P\{^1H\}$ NMR spectrum featured an AB quartet ($\delta=102.7$ and 99.1 ppm, $J_{AB}=89.1$ Hz), implying that the molecular symmetry was broken. Similar results were obtained when HCl and glacial acetic acid were employed. Pyrrole-type molecules are known to undergo protonation at the α- or β-carbons,[17] and both types of protonation reactions have been observed by Nishibayashi and co-workers in their studies of (^{tBu}PNP)$Fe(N_2)$ and the related compounds.[12a,c] To discern the exact site for the protonation, a preparative-scale reaction of **1** with $HBF_4\cdot Et_2O$ was performed, and the isolated product *cis*-[(H^{Cy}PNP)$Fe(CO)_2H]BF_4$ (**4**, H^{Cy}PNP stands for a protonated PNP-pincer ligand) was studied by X-ray crystallography (Figure 2). Although the extent of disorder (see Supporting Information) does not permit a detailed structural analysis, the bond metrics for the pyrrolyl ring can be interpreted with high confidence. For example, the C3–C4 and C5–C4 bonds

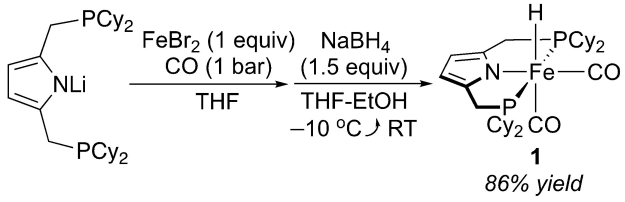

Scheme 1. One-pot synthesis of *cis*-(^{Cy}PNP)$Fe(CO)_2H$ (**1**).

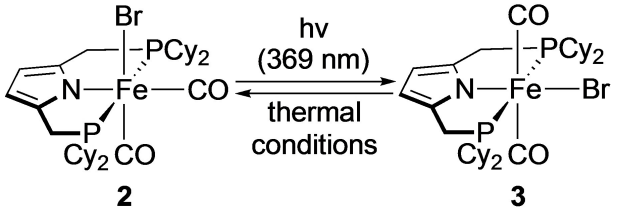

Scheme 2. Isomerization of *cis*- and *trans*-(^{Cy}PNP)$Fe(CO)_2Br$.

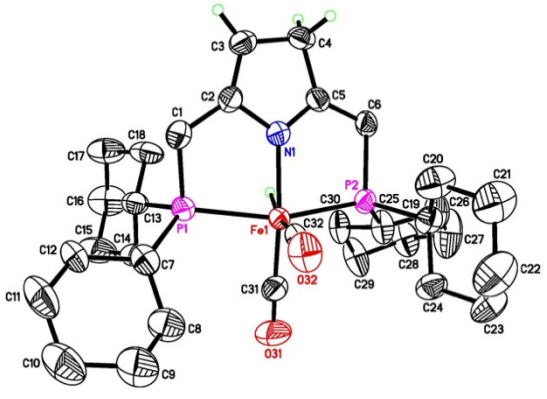

Figure 2. ORTEP drawing of the cation in *cis*-[(H^{Cy}PNP)$Fe(CO)_2H]BF_4$ (**4**) at the 50% probability level (all hydrogen atoms except the hydride and those bound to C3 and C4 omitted for clarity).[19]

(1.492(6) and 1.491(5) Å, respectively) are considerably longer than the C2–C3 bond (1.323(6) Å) and should be categorized as C_{sp2}–C_{sp3} single bonds. The C5–N1 bond (1.298(5) Å) is best described as a double bond, further confirming that protonation has occurred to the β-carbon, which is analogous to an enamine-to-iminium conversion.[18] Additional spectroscopic evidence supporting the structure includes only one aromatic/vinylic hydrogen present in the ^{1}H NMR spectrum (6.40 ppm, in C_6D_6) and an iminium-type carbon resonance observed at 187.8 ppm as a doublet of doublets ($J_{C\text{-}P}$ = 7.2 and 4.4 Hz).

Upon conversion of **1** to **4**, the hydride resonance is shifted slightly from −7.37 to −7.51 ppm, appearing as an apparent triplet despite the broken symmetry. The hydride signal persists even if $HBF_4 \cdot Et_2O$ is added in excess, which is quite unusual for an iron hydride. The protonation process is reversible, as **4** is readily converted back to **1** via addition of a weak base such as Et_3N (Scheme 3). Furthermore, the hydrogens on the β-carbons are exchangeable with CD_3OD when **1** is dissolved in CD_3OD/C_6D_6 (50:50). In contrast, the hydride does not undergo H/D exchange with CD_3OD. The mechanism by which **1** reduces PhCHO to $PhCH_2OH$ assisted by $HBF_4 \cdot Et_2O$ remains unclear to us; however, it is conceivable that the in-situ generated **4** transfers H^+ and H^- stepwise to PhCHO following an ionic hydrogenation pathway.[20]

According to the ligand acidity constant method developed by Morris,[21] the presence of CO ligands can drastically increase the acidity of a metal dihydrogen or hydride complex. One would predict that the dihydrogen complex, if formed from protonation of **1**, would be exceptionally acidic. This is likely contributing to the failure of **1** to undergo protonation at the hydride site. Similarly, **1** itself is expected to be relatively acidic because of the two CO ligands, and K[(^{Cy}PNP)Fe(CO)$_2$] is a known compound.[9a] However, no deprotonation of **1** was observed when it was treated with KO^{t}Bu in THF.

One could perhaps be convinced that the iron hydride **1**, an 18-electron complex, needs to dissociate a CO ligand first in order to exhibit hydride reactivity, which may be achieved under UV irradiation. Although the bromide complex **2** was shown to isomerize to its *trans* isomer **3** under the photochemical conditions, **1** did not share this propensity. However, exposure of **1** to ethylene resulted in a slow conversion of **1** to a previously known iron ethyl complex, *cis*-(^{Cy}PNP)Fe(CO)$_2$Et (Scheme 4).[9a]

In addition to the aforementioned insertion chemistry, H/D exchange between the hydride and C_6D_6 was also observed, as evidenced by a 1:1:1 triplet (101.1 ppm) emerging in the ^{31}P{^{1}H} NMR spectrum. This resonance can be attributed to the iron deuteride **1-D** (isotopically shifted from **1** by 0.1 ppm), which was independently synthesized from **2** and $NaBD_4$ in EtOD. As expected, the H/D exchange process can take place without ethylene (Scheme 5). Under similar conditions, **1** was shown to exchange its hydride with deuterium atoms in toluene-d_8 but only with those on the sp^2 carbons. A series of control experiments were then conducted to provide the following mechanistic insights: (1) the H/D exchange process depicted in Scheme 5 is minimally inhibited by CO (1 bar); (2) under ambient conditions, **1** does not exchange with ^{13}CO (1 bar); and (3) under UV irradiation, ^{13}CO is incorporated into **1** at a rate significantly faster than H/D exchange. These results support a mechanism involving photodissociation of CO from **1** to generate a minute amount of (^{Cy}PNP)Fe(CO)H, which in turn activates the C_{sp2}–D bonds in the solvent molecule to initiate the H/D exchange process. The intermediate (^{Cy}PNP)Fe(CO)H must also be responsible for ethylene insertion described earlier.

To test the hypothesis that a radical chain mechanism might be involved in the H/D exchange process, galvinoxyl was used as a radical scavenger. It quickly became obvious that galvinoxyl reacts rapidly with **1**, without UV irradiation, to give a new iron hydride complex, as indicated by a proton resonance located at −7.65 ppm (t, $J_{C\text{-}P}$ = 47.4 Hz, in C_6D_6). The stoichiometry of the reaction was determined to be 2:1, suggesting that two hydrogen atoms per molecule of **1** are transferred to galvinoxyl. The related species, the 2,4,6-tri-*tert*-butylphenoxy radical, has been reported to dehydrogenate or oxidize the pincer backbone in cobalt and nickel complexes supported by a $[N(CH_2CH_2PR_2)_2]^-$ ligand.[22]

An alternative reagent used for this purpose is 1,4-benzoquinone (only 1 equiv. required),[22a,23] which has been employed to oxidize the pincer backbone in (^{tBu}PNP)MCl (M = Ni, Co).[24] However, such a strategy is unsuccessful with the analogous iron complex (^{tBu}PNP)FeCl, which has been attributed to oxidation of the iron center.[24] Given this result, it was particularly interesting to find that mixing **1** with 1,4-benzoqui-

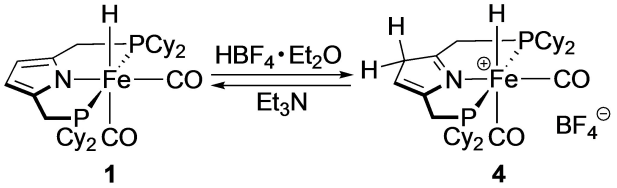

Scheme 3. Reversible protonation of *cis*-(^{Cy}PNP)Fe(CO)$_2$H (**1**).

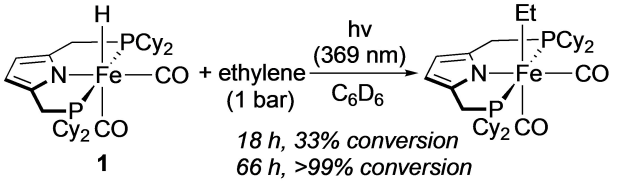

Scheme 4. Insertion of ethylene under UV irradiation.

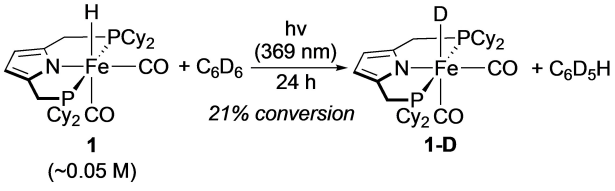

Scheme 5. H/D exchange between *cis*-(^{Cy}PNP)Fe(CO)$_2$H (**1**) and C_6D_6.

none (Scheme 6) produced the same iron hydride obtained from the galvinoxyl reaction. The isolated product, *cis*-(^{Cy}PNP*)Fe(CO)$_2$H (**5**, ^{Cy}PNP* stands for a dehydrogenated PNP-pincer ligand), differs spectroscopically from **1**. The most notable change in the ^{1}H NMR spectra (in C_6D_6) is the disappearance of the diastereotopic hydrogens ($\delta = 3.03$ and 2.95 ppm) for the CH_2 groups adjacent to the phosphorus donors, replaced by vinylic-type hydrogens ($\delta = 4.33$ ppm) appearing as a virtual triplet. The loss of a total of two hydrogen atoms was further confirmed by mass spectrometry (ESI-MS). Previous studies of 2,5-bis(oxazolinylmethyl)pyrrole-based pincer complexes suggest that the methylene linkages can readily lose a hydrogen, leading to a more delocalized π-system for the pincer scaffold.[25] Perhaps this is also the driving force for the reaction shown in Scheme 6. Nevertheless, the fact that the Fe–H bond can survive the oxidizing conditions is noteworthy, highlighting the robustness of the hydride moiety.

Conclusions

Through this work, we have demonstrated primarily ligand-based reactivity for an iron hydride complex. The presence of a pyrrole-based PNP-pincer ligand along with two CO ligands render the Fe–H bond exceptionally stable (or unreactive). Protonation with a strong acid occurs at the β-pyrrolic carbon, and oxidation with 1,4-benzoquinone or galvinoxyl results in dehydrogenation of the pincer backbone, leaving the Fe–H bond intact. Under photochemical conditions, CO can dissociate from iron, allowing ethylene to insert into the Fe–H bond and C_6D_6 to exchange H/D with the hydride. These results add to the understanding of pyrrole-based pincer complexes,[26] which have the potential to be developed as catalysts involving metal-ligand cooperation.[27]

Experimental Section

General: All iron complexes described in this paper were prepared under an argon atmosphere using standard glovebox and Schlenk techniques. Benzene-d_6 was dried over sodium-benzophenone and distilled under an argon atmosphere. Ethanol was dried over 3 Å molecular sieves and then deoxygenated by bubbling argon through it for 10 min. Benzene was not dried but was deoxygenated by bubbling argon through it for 10 min. All other dry and oxygen-free solvents used for synthesis and workup (THF, Et_2O, toluene, and pentane) were collected from an Innovative Technology solvent purification system. Li(^{Cy}PNP) was prepared according to a literature procedure.[14] Chemical shift values in ^{1}H and ^{13}C{^{1}H} NMR spectra were referenced internally to the residual solvent resonances. ^{31}P{^{1}H} spectra were referenced externally to 85% H_3PO_4 (0 ppm). Infrared spectra were recorded on a PerkinElmer Spectrum Two FT-IR spectrometer equipped with a smart orbit diamond attenuated total reflectance (ATR) accessory.

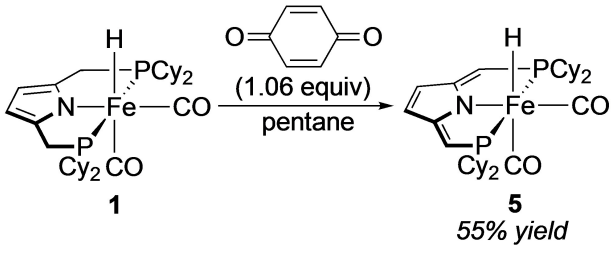

Scheme 6. Reaction of *cis*-(^{Cy}PNP)Fe(CO)$_2$H (**1**) with 1,4-benzoquinone.

Synthesis of *cis*-(^{Cy}PNP)Fe(CO)$_2$H (1): This complex has been previously reported by Tonzetich and co-workers,[9a] though involving a synthetic protocol different from ours described herein. Under an argon atmosphere, a 50 mL oven-dried Schlenk flask equipped with a stir bar was charged with Li(^{Cy}PNP) (1.00 g, 2.03 mmol) and anhydrous $FeBr_2$ (437 mg, 2.03 mmol). The argon was removed under vacuum and replaced with CO gas (1 bar). Dry THF (20 mL) was then added with stirring. The resulting dark red solution was stirred under CO (1 bar) for 30 min, at which point the atmosphere was switched back to argon and the dark red solution was cooled to −10 °C. A 0.1 M solution of $NaBH_4$ in EtOH was added dropwise (15.2 mL, 1.52 mmol) and the reaction mixture was gradually warmed to room temperature and stirred for 1 h. The green-brown solution was cooled again to −10 °C and a second portion of $NaBH_4$ was added (15.2 mL, 1.52 mmol). The reaction mixture was again gradually warmed to room temperature and stirred for 16 h. Removal of volatiles under vacuum produced a dark green-brown oil, which was dissolved in toluene (10 mL) and then filtered through a pad of Celite followed by toluene elution (10 mL × 2). The combined toluene solutions were evaporated to dryness, and the resulting oil was triturated with pentane (10 mL), which was then decanted. The residual pentane was removed under vacuum to afford the desired product as a pale-green powder (1.04 g, 86% yield). ^{1}H NMR, ^{31}P{^{1}H} NMR, and IR data match those previously reported.[9a] X-ray quality crystals (orange color) were grown from diethyl ether. **^{1}H NMR** (400 MHz, C_6D_6): $\delta = 6.48$ (s, 2H, pyrrole C*H*), 3.03 (AB, $J_{AB} = 16.0$ Hz, 2H, PCH_2), 2.95 (AB of vt, $J_{AB} = 16.0$ Hz, $J = 5.2$ Hz, 2H, PCH_2), 2.09–1.83 (m, 10H, Cy*H*), 1.73–1.52 (m, 16H, Cy*H*), 1.47–1.33 (m, 6H, Cy*H*), 1.20–1.03 (m, 12H, Cy*H*), −7.37 (t, $J_{H\text{-}P} = 48.8$ Hz, 1H, Fe*H*). **^{31}P{^{1}H} NMR** (162 MHz, C_6D_6): $\delta = 100.94$ (s). **IR** (solid, ATR): 2926 m, 2849 m, 1981 s (ν_{CO}), 1920 s (ν_{CO}), 1446 m, 1384 w, 1341 w, 1266 w cm^{-1}. **ESI-MS**: *m/z* = 600.33 ([M + H]$^+$, 100%), 572.42 ([M + H–CO]$^+$, 22%), 544.42 ([M + H–2CO]$^+$, 11%).

Synthesis of *cis*-(^{Cy}PNP)Fe(CO)$_2$Br (2): Under an argon atmosphere, a 25 mL oven-dried Schlenk flask equipped with a stir bar was charged with Li(^{Cy}PNP) (500 mg, 1.01 mmol) and anhydrous $FeBr_2$ (218 mg, 1.01 mmol). The argon was removed under vacuum and replaced with CO gas (1 bar). Dry THF (10 mL) was then added with stirring. The resulting dark red solution was stirred under CO (1 bar) for 30 min, at which point the atmosphere was switched back to argon and the reaction mixture was stirred for 16 h. Removal of volatiles under vacuum gave an orange solid, which was treated with toluene (10 mL) and then filtered through a pad of Celite followed by toluene elution (10 mL × 2). The combined toluene solutions were evaporated to dryness to afford the desired product as an orange powder (661 mg, 96% yield). X-ray quality crystals were grown from toluene-pentane. $C_{32}H_{50}BrFeNO_2P_2$ (678.44): C 56.77 (calc. 56.65); H 7.63 (7.43); N 2.14 (2.06)%. **^{1}H NMR** (400 MHz, C_6D_6): $\delta = 6.57$ (s, 2H, pyrrole C*H*), 3.46 (AB of vt, $J_{AB} = 11.6$ Hz, $J = 5.2$ Hz, 2H, PCH_2), 3.18–2.99 (m, 4H, PC*H* and PCH_2), 2.41–2.32 (m, 2H, Cy CH_2), 2.07–1.98 (m, 2H, PC*H*), 1.96–1.85 (m, 4H, Cy CH_2), 1.83–1.77 (m, 2H, Cy CH_2), 1.72–1.66 (m, 2H, Cy CH_2), 1.64–1.45 (m, 16H, Cy CH_2), 1.42–1.31 (m, 4H, Cy CH_2), 1.15–0.92 (m, 10H, Cy CH_2). **^{13}C{^{1}H} NMR** (101 MHz, C_6D_6): $\delta = 216.14$ (t, $J_{C\text{-}P} = 23.9$ Hz, *C*O), 214.97 (t, $J_{C\text{-}P} = 15.6$ Hz, *C*O), 134.77 (vt, $J = 4.0$ Hz, pyrrole α-*C*), 106.72 (vt, $J = 4.5$ Hz, pyrrole β-*C*), 37.90 (vt, $J = 8.6$ Hz, PCH), 36.90 (vt, $J = 9.3$ Hz, PCH), 30.06 (s, Cy *C*H$_2$), 29.92 (s, Cy *C*H$_2$), 29.42 (s, Cy *C*H$_2$), 29.39 (s,

Cy CH_2), 27.75 (vt, J = 13.1 Hz, PCH_2), 27.54 (vt, J = 5.9 Hz, Cy CH_2), 27.50 (vt, J = 5.2 Hz, Cy CH_2), 27.29 (vt, J = 4.8 Hz, Cy CH_2), 27.24 (vt, J = 5.1 Hz, Cy CH_2), 26.41 (s, Cy CH_2), 26.17 (s, Cy CH_2). **^{31}P{^{1}H} NMR** (162 MHz, C_6D_6): δ = 78.57 (s). **IR** (solid, ATR): 2925 m, 2850 m, 2008 s (ν_{CO}), 1947 s (ν_{CO}), 1444 m, 1377 w, 1264 w cm^{-1}. **ESI-MS**: *m/z* = 678.17 ([M + H]$^+$, 5%), 598.08 ([M − Br]$^+$, 100%), 570.17 ([M − Br − CO]$^+$, 16%), 542.42 ([M − Br − 2CO]$^+$, 3%).

Photogeneration of *trans*-(^{Cy}PNP)Fe(CO)$_2$Br (3): Under an argon atmosphere, **2** (15 mg, 22 μmol) was mixed with C_6D_6 (0.5 mL) in a J. Young NMR tube. The resulting solution was degassed via three freeze-pump-thaw cycles and then placed under a ^{13}CO atmosphere (1 bar). The NMR tube was irradiated with an array of four 369 nm UV-LEDs (at room temperature) for 1 h, after which the NMR spectra were recorded. Selected **^{13}C{^{1}H} NMR** data (101 MHz, C_6D_6): δ = 218.22 (t, $J_{C\text{-}P}$ = 23.2 Hz, ^{13}CO in **3-^{13}CO** and **3-(^{13}CO)$_2$**), 184.51 (s, free ^{13}CO). **^{31}P{^{1}H} NMR** (162 MHz, C_6D_6): δ = 78.59 (s, **2**, 35% of total P-containing species), 69.67 (overlapping singlet, doublet, and triplet for **3**, **3-^{13}CO**, and **3-(^{13}CO)$_2$**, respectively, $J_{P\text{-}C}$ = 23.2 Hz). A mixture of **2** and **3** was generated from pure **2** under photochemical conditions described above except under an argon atmosphere. The ν_{CO} band of **3** was not located due to overlapping with the ν_{CO} bands of **2**.

Synthesis of *cis*-[(H^{Cy}PNP)Fe(CO)$_2$H]BF$_4$ (4): Under an argon atmosphere, a 10 mL Schlenk tube equipped with a stir bar was charged with **1** (100 mg, 0.17 mmol) and benzene (3 mL). The resulting solution was treated with $HBF_4 \cdot Et_2O$ (25.3 μL, 0.18 mmol), resulting in an immediate color change from pale green to yellow. A brief vacuum was applied to remove the majority of the benzene and the resulting orange oil was dissolved in EtOH (2 mL). Subsequent addition of pentane (10 mL) caused a dark oily precipitate to deposit on the sides of the flask. The solution was decanted, and pentane was added until persistent cloudiness (10 mL). The mixture was placed in a freezer at −27 °C for 24 h and yellow crystals developed, which were suitable for X-ray crystallographic study. The solvent was then decanted, and the crystals were allowed to dry for 24 h under a gentle argon stream (20 mg, 17% yield). $C_{32}H_{52}FeNO_2P_2BF_4$ (687.36): C 56.40 (calc. 55.92); H 7.90 (7.63); N 2.01 (2.04)%. **^{1}H NMR** (400 MHz, C_6D_6): δ = 6.40 (s, 1H, C*H*=C–N), 4.13–3.78 (m, 2H), 3.68–3.35 (m, 2H), 3.06–2.77 (m, 1H), 2.60–2.35 (m, 1H), 2.18–1.84 (m, 8H), 1.84–1.52 (m, 14H), 1.51–1.05 (m, 22H), −7.51 (t, $J_{H\text{-}P}$ = 46.2 Hz, 1H, Fe*H*). **^{13}C{^{1}H} NMR** (101 MHz, C_6D_6): δ = 215.30 (t, $J_{C\text{-}P}$ = 18.6 Hz, *C*O), 209.46 (t, $J_{C\text{-}P}$ = 10.3 Hz, *C*O), 187.76 (dd, $J_{C\text{-}P}$ = 7.2 and 4.4 Hz, *C*=N), 151.77 (dd, $J_{C\text{-}P}$ = 4.8 and 3.3 Hz, CH=*C*–N), 120.40 (d, $J_{C\text{-}P}$ = 9.1 Hz, *C*H=C–N), 48.25 (d, $J_{C\text{-}P}$ = 5.9 Hz, *C*H$_2$–C=N), 39.32 (d, $J_{C\text{-}P}$ = 19.8 Hz, P*C*H), 39.28 (d, $J_{C\text{-}P}$ = 21.7 Hz, P*C*H), 36.57 (d, $J_{C\text{-}P}$ = 21.3 Hz, P*C*H), 36.32 (d, $J_{C\text{-}P}$ = 21.0 Hz, P*C*H), 33.65 (d, $J_{C\text{-}P}$ = 23.3 Hz, P*C*H$_2$C=N), 29.57 (s, Cy *C*H$_2$), 29.36 (s, Cy *C*H$_2$), 29.22 (s, Cy *C*H$_2$), 29.02 (s, Cy *C*H$_2$), 28.98 (s, Cy *C*H$_2$), 27.92 (s, Cy *C*H$_2$); 9 doublets and 6 singlets are expected in the 27.8–26.0 ppm region, which is too crowded to make a definitive assignment. **^{31}P{^{1}H} NMR** (162 MHz, C_6D_6): δ = 102.72 (AB, J_{AB} = 89.1 Hz), 99.09 (AB, J_{AB} = 89.1 Hz). **IR** (solid, ATR): 2923 m, 2851 w, 1998 s (ν_{CO}), 1948 s (ν_{CO}), 1447 w, 1045 s cm^{-1}. **ESI-MS**: *m/z* = 600.25 ([M − BF$_4$]$^+$, 100%), 572.33 ([M − BF$_4$ − CO]$^+$, 5%).

Synthesis of *cis*-(^{Cy}PNP)Fe(CO)$_2$D (1-D): This complex (93% D on Fe) was synthesized from **2** and $NaBD_4$ in EtOD. The β-pyrrolic carbon was partially deuterated, as judged by ^{1}H and ^{2}H NMR spectroscopy. **^{31}P{^{1}H} NMR** (162 MHz, C_6D_6): δ = 101.01 (t, $J_{P\text{-}D}$ = 7.0 Hz).

Synthesis of *cis*-(^{Cy}PNP*)Fe(CO)$_2$H (5): Under an argon atmosphere, a 50 mL Schlenk tube equipped with a stir bar was charged with **1** (100 mg, 0.17 mmol) and pentane (25 mL). 1,4-benzoquinone (19 mg, 0.18 mmol) was added, resulting in a color change from pale green to dark red. The reaction mixture was stirred at room temperature for 30 min before being cooled to −78 °C. Filtration performed at this temperature yielded a dark red solution and a black solid. The solid was mixed with pentane (10 mL), which was also filtered at −78 °C. Removal of the volatiles from the combined pentane solutions afforded the desired product as a red powder (55 mg, 55% yield). $C_{32}H_{49}FeNO_2P_2$ (597.53): C 64.84 (calc. 64.32); H 8.29 (8.27); N 2.26 (2.34)%. **^{1}H NMR** (400 MHz, C_6D_6): δ = 6.64 (s, 2H, C*H*=C*H*), 4.33 (vt, J = 2.8 Hz, 2H, PC*H*=C–N), 2.23–2.12 (m, 8H, Cy*H*), 1.96–1.84 (m, 4H, Cy*H*), 1.81–1.55 (m, 22H, Cy*H*), 1.26–1.16 (m, 10H, Cy*H*), −7.65 (t, $J_{H\text{-}P}$ = 47.4 Hz, 1H, Fe*H*). **^{13}C{^{1}H} NMR** (101 MHz, C_6D_6): δ = 218.04 (t, $J_{C\text{-}P}$ = 18.0 Hz, *C*O), 212.17 (t, $J_{C\text{-}P}$ = 12.1 Hz, *C*O), 168.94 (vt, J = 12.7 Hz, PCH=*C*–N), 132.18 (vt, J = 6.7 Hz, *C*H=CH), 82.03 (vt, J = 20.4 Hz, PCH=C–N), 40.77 (vt, J = 11.7 Hz, P*C*H), 39.47 (vt, J = 13.9 Hz, P*C*H), 30.58 (s, Cy *C*H$_2$), 30.30 (s, Cy *C*H$_2$), 29.99 (s, Cy *C*H$_2$), 29.19 (s, Cy *C*H$_2$), 27.96 (vt, J = 6.2 Hz, Cy *C*H$_2$), 27.75–27.73 (m, Cy *C*H$_2$), 26.89 (s, Cy *C*H$_2$), 26.66 (s, Cy *C*H$_2$). **^{31}P{^{1}H} NMR** (162 MHz, C_6D_6): δ = 103.84 (s). **IR** (solid, ATR): 2921 m, 2849 m, 1983 s (ν_{CO}), 1926 s (ν_{CO}), 1867 w, 1538 s, 1446 m, 1446 m cm^{-1}. **ESI-MS**: *m/z* = 598.25 ([M + H]$^+$, 100%).

X-ray structure determinations: Crystal data collection and refinement parameters are provided in the Supporting Information. Intensity data for **1**·1/2Et$_2$O were collected at 150 K on a Bruker D8 APEX-II CCD diffractometer using Mo Kα radiation, λ = 0.71073 Å. Intensity data for **2** and **4** were collected at 150 K on a Bruker D8 Venture Photon-II diffractometer using Mo Kα radiation, λ = 0.71073 Å. The data frames were processed using the program SAINT. The data were corrected for decay, Lorentz, and polarization effects as well as absorption and beam corrections based on the multi-scan technique. The structures were solved by a combination of direct methods and the difference Fourier technique as implemented in the SHELX suite of programs and refined by full-matrix least-squares on F^2. Non-hydrogen atoms were refined with anisotropic displacement parameters. For **1**, a disordered half-molecule of diethyl ether crystallizes in the lattice. Anisotropic displacement parameters for the carbonyl groups in **1**·1/2Et$_2$O were refined as equivalent. The hydride in **1**·1/2Et$_2$O was located directly from the difference map and the coordinates were refined. All remaining hydrogen atoms were calculated and treated with a riding model. In **2**, the *trans* bromide and carbonyl are disordered, occupancy set at 0.5. Distance restraints were applied to the C20/O20 atoms so that they correspond more closely to the C19/O19 atoms. The ligand backbone has unresolved disorder with the elongated displacement parameters for the symmetry-related C3–C3 A pair. As a result, the bond between them is shorter than is typical for a C–C single bond. Attempts to model with a multi-component model did not yield satisfactory results. Disorder is also observed in a cyclohexyl ring (C13–C18), a two-component model was refined with the occupancy refined (major occupancy = 67%). Complex **4** crystallizes with two independent molecules in the lattice along with a disordered pentane molecule. However, due to the degree of disorder, the solvent contribution was removed from the reflection data using Squeeze as implemented in PLATON. The *trans* hydride and carbonyl are disordered, and the occupancy was refined. The major component of the hydride was located but the position was not refined. The minor component of the hydride was not located but can be inferred based on the carbonyl positions. Disorder is also observed in the iron positions and the cyclohexyl rings; two-component disorder models were applied, and the occupancies were refined. Hydrogen atoms were calculated and treated with a riding model. The hydrogen atom isotropic displacement parameters were defined as 1.2*U$_{eq}$ of the adjacent atom.

Crystallographic data for the structures in this paper have been deposited with the Cambridge Crystallographic Data Centre, CCDC, 12 Union Road, Cambridge CB21EZ, UK. Copies of the data can be obtained free of charge on quoting the depository numbers CCDC-

2064210, CCDC-2064211, and CCDC-2064212 for **1**·1/2Et_2O, **2**, and **4**, respectively (Fax: +44-1223-336-033; E-Mail: deposit@ccdc.cam.ac.uk, http://www.ccdc.cam.ac.uk)

Acknowledgements

We thank the NSF Chemical Catalysis Program (CHE-1800151) and MRI Program (CHE-0215950 and CHE-1625737) for support of this research.

Keywords: Iron · Hydrides · Phosphines · Protonation · Oxidation

[1] W. Hieber, F. Leutert, *Naturwissenschaften* **1931**, *19*, 360–361.
[2] a) H. Nakazawa, M. Itazaki, *Top. Organomet. Chem.* **2011**, *33*, 27–81; b) H. Dai, H. Guan, *Isr. J. Chem.* **2017**, *57*, 1170–1203.
[3] a) P. Bhattacharya, H. Guan, *Comments Inorg. Chem.* **2011**, *32*, 88–112; b) T. Zell, D. Milstein, *Acc. Chem. Res.* **2015**, *48*, 1979–1994; c) A. Saini, M. Findlater, in: *Pincer Compounds: Chemistry and Applications* (Ed.: D. Morales-Morales), Elsevier, Amsterdam **2018**, pp. 327–339; d) W. D. Jones, *Top. Organomet. Chem.* **2019**, *63*, 141–174.
[4] a) C. Gunanathan, D. Milstein, *Acc. Chem. Res.* **2011**, *44*, 588–602; b) H. Li, B. Zheng, K.-W. Huang, *Coord. Chem. Rev.* **2015**, *293–294*, 116–138; c) D. Benito-Garagorri, K. Kirchner, *Acc. Chem. Res.* **2018**, *41*, 201–213; d) H. Li, T. P. Gonçalves, D. Lupp, K.-W. Huang, *ACS Catal.* **2019**, *9*, 1619–1629.
[5] a) S. Schneider, J. Meiners, B. Askevold, *Eur. J. Inorg. Chem.* **2012**, *2012*, 412–429; b) W. H. Bernskoetter, N. Hazari, in: *Pincer Compounds: Chemistry and Applications* (Ed.: D. Morales-Morales), Elsevier, Amsterdam **2018**, pp. 111–131; c) Z. Wei, H. Jiao, *Adv. Inorg. Chem.* **2019**, *73*, 323–384; d) D. A. Ekanayake, H. Guan, *Top. Organomet. Chem.* **2021**, *68*, 263–320.
[6] N. Grüger, H. Wadepohl, L. H. Gade, *Dalton Trans.* **2012**, *41*, 14028–14030.
[7] S. Kumar, G. Mani, S. Mondal, P. K. Chattaraj, *Inorg. Chem.* **2012**, *51*, 12527–12539.
[8] G. T. Venkanna, T. V. M. Ramos, H. D. Arman, Z. J. Tonzetich, *Inorg. Chem.* **2012**, *51*, 12789–12795.
[9] a) C. V. Thompson, H. D. Arman, Z. J. Tonzetich, *Organometallics* **2017**, *36*, 1795–1802; b) T. Kato, S. Kuriyama, K. Nakajima, Y. Nishibayashi, *Chem. Asian J.* **2019**, *14*, 2097–2101.
[10] C. V. Thompson, I. Davis, J. A. DeGayner, H. D. Arman, Z. J. Tonzetich, *Organometallics* **2017**, *36*, 4928–4935.
[11] C. V. Thompson, H. D. Arman, Z. J. Tonzetich, *Organometallics* **2019**, *38*, 2979–2989.
[12] a) S. Kuriyama, K. Arashiba, K. Nakajima, Y. Matsuo, H. Tanaka, K. Ishii, K. Yoshizawa, Y. Nishibayashi, *Nat. Commun.* **2016**, *7*, 12181; b) K. Nakajima, T. Kato, Y. Nishibayashi, *Org. Lett.* **2017**, *19*, 4323–4326; c) Y. Sekiguchi, S. Kuriyama, A. Eizawa, K. Arashiba, K. Nakajima, Y. Nishibayashi, *Chem. Commun.* **2017**, *53*, 12040–12043.
[13] a) P. Bhattacharya, J. A. Krause, H. Guan, *Organometallics* **2011**, *30*, 4720–4729; b) P. Bhattacharya, J. A. Krause, H. Guan, *Organometallics* **2014**, *33*, 6113–6121.
[14] S. Kuriyama, K. Arashiba, H. Tanaka, Y. Matsuo, K. Nakajima, K. Yoshizawa, Y. Nishibayashi, *Angew. Chem.* **2016**, *128*, 14503–14507; *Angew. Chem. Int. Ed.* **2016**, *55*, 14291–14295.
[15] The crystals grown for X-ray crystallographic study are orange, implying that the pale green color noted for the bulk material may be due to the presence of a very small amount of (^{Cy}PNP)$Fe(CO)_2$, which was reported as a blue solid.[9a].
[16] A limited number of scans were applied so that only the ^{13}C-labelled species could be observed by $^{13}C\{^1H\}$ NMR spectroscopy.
[17] J. Catalán, M. Yáñez, *J. Am. Chem. Soc.* **1984**, *106*, 421–422.
[18] H. Guan, M. Iimura, M. P. Magee, J. R. Norton, G. Zhu, *J. Am. Chem. Soc.* **2005**, *127*, 7805–7814.
[19] Compound **4** crystallizes with two independent molecules in the lattice. Each shows disorder with the hydride, its *trans* CO ligand, the iron position, and the cyclohexyl rings. Only the major component of one molecule is shown here.
[20] R. M. Bullock, *Chem. Eur. J.* **2004**, *10*, 2366–2374.
[21] a) R. H. Morris, *J. Am. Chem. Soc.* **2014**, *136*, 1948–1959; b) M. M. H. Sung, R. H. Morris, *Inorg. Chem.* **2016**, *55*, 9596–9601; c) J. P. Unsleber, J. Neugebauer, R. H. Morris, *Dalton Trans.* **2018**, *47*, 2739–2747.
[22] a) P. O. Lagaditis, B. Schluschaß, S. Demeshko, C. Würtele, S. Schneider, *Inorg. Chem.* **2016**, *55*, 4529–4536; b) F. Schneck, M. Finger, M. Tromp, S. Schneider, *Chem. Eur. J.* **2017**, *23*, 33–37.
[23] N. P. N. Wellala, J. D. Luebking, J. A. Krause, H. Guan, *ACS Omega* **2018**, *3*, 4986–5001.
[24] V. M. Krishnan, I. Davis, T. M. Baker, D. J. Curran, H. D. Arman, M. L. Neidig, A. Liu, Z. J. Tonzetich, *Inorg. Chem.* **2018**, *57*, 9544–9553.
[25] a) C. Mazet, L. H. Gade, *Chem. Eur. J.* **2003**, *9*, 1759–1767; b) F. Konrad, J. L. Fillol, C. Rettenmeier, H. Wadepohl, L. H. Gade, *Eur. J. Inorg. Chem.* **2009**, *2009*, 4950–4961; c) F. Konrad, J. L. Fillol, H. Wadepohl, L. H. Gade, *Inorg. Chem.* **2009**, *48*, 8523–8535; d) C. Rettenmeier, H. Wadepohl, L. H. Gade, *Chem. Eur. J.* **2014**, *20*, 9657–9665.
[26] C. V. Thompson, Z. J. Tonzetich, *Adv. Organomet. Chem.* **2020**, *74*, 153–240.
[27] T. P. Gonçalves, I. Dutta, K.-W. Huang, *Chem. Commun.* **2021**, *57*, 3070–3082.

Manuscript received: February 23, 2021
Revised manuscript received: March 29, 2021
Accepted manuscript online: March 30, 2021